

## Covariant calculation of mesonic baryon decays

T. Melde, W. Plessas, and R. F. Wagenbrunn

*Theoretical Physics, Institute for Physics, University of Graz, Universitätsplatz 5, A-8010 Graz, Austria*

(Received 24 March 2005; published 21 July 2005)

We present covariant predictions for  $\pi$  and  $\eta$  decay modes of  $N$  and  $\Delta$  resonances from relativistic constituent-quark models based on one-gluon-exchange and Goldstone-boson-exchange dynamics. The results are calculated within the point-form approach to Poincaré-invariant relativistic quantum mechanics applying a spectator-model decay operator. The direct predictions of the constituent-quark models for covariant  $\pi$  and  $\eta$  decay widths show a behavior completely different from previous ones calculated in nonrelativistic or so-called semirelativistic approaches. The present theoretical results agree with experiment only in a few cases but otherwise always remain smaller than the experimental data (as compiled by the Particle Data Group). Possible reasons for this behavior are discussed with regard to the quality of both the quark-model wave functions and the mesonic decay operator.

DOI: [10.1103/PhysRevC.72.015207](https://doi.org/10.1103/PhysRevC.72.015207)

PACS number(s): 12.39.Ki, 13.30.Eg

### I. INTRODUCTION

Hadronic transitions between baryon states represent a wide field of physical phenomena to be understood ultimately on the basis of quantum chromodynamics (QCD), the fundamental theory of strong interactions. While there is a wealth of experimental data available, theory lags behind with regard to a comprehensive explanation. This is mainly due to the persisting difficulties of solving QCD rigorously in the low- and intermediate-energy regimes. There one has to resort to effective theories or models based as far as possible on the genuine properties of QCD. Furthermore, they should provide a comprehensive framework covering also other hadron phenomena (e.g., interactions with electroweak probes, etc.). The quark-model description of light and strange baryons has seen a number of interesting and important new developments over the last few years. In addition to the traditional constituent-quark model (CQM), whose hyperfine interaction derives from one-gluon exchange (OGE) [1], alternative types of CQMs have been suggested such as those based on instanton-induced (II) forces [2,3] or Goldstone-boson-exchange (GBE) dynamics [4]. The GBE CQM [5,6] aims at incorporating the basic properties of low-energy QCD, as following from the spontaneous breaking of chiral symmetry ( $SB\chi S$ ).

Properties of baryon resonances should be calculated in a fully relativistic approach. In this paper, the theory is formulated along relativistic, i.e., Poincaré-invariant, quantum mechanics [7]. Specifically, we adhere to its point-form version [8,9], since this allows us to calculate observables in a manifestly covariant manner [10]. This approach is *a priori* distinct from a field-theoretic treatment. It relies on a relativistically invariant mass operator with the interactions included according to the Bakamjian-Thomas construction [11]. In this way, all the required symmetries of special relativity can be fulfilled. Relativistic CQMs have already been applied in the description of electroweak nucleon form factors [12–17] and electric radii as well as magnetic moments of all octet and decuplet baryon ground states [18,19]. In this context, the point-form approach has turned out surprisingly successful.

Here we are interested in determining if an analogous treatment of strong decays also leads to a satisfactory description of this type of hadronic reaction, in agreement with existing experimental data.

Mesonic resonance decays have always been considered as a big challenge, with early attempts dating back to the 1960s [20–24]. With the refinement of CQMs over the years, more studies on different aspects of mesonic decays have been performed. In the course of the past two decades, a number of valuable insights have thus been gained by various groups, e.g., in Refs. [25–33]. The focus of interest has been, notably, the performance of various CQMs as well as the adequacy of different decay operators for the mechanism of meson creation/emission. Despite the considerable efforts invested, we still do not have a satisfactory microscopic explanation of especially the  $N$  and  $\Delta$  resonance decays. Also, complementary attempts outside the CQM approach have not had much more success with hadron decays or, more generally, with providing a comprehensive working model of low-energy hadronic physics based on QCD. This situation is rather unsatisfactory from the theoretical side, especially in view of the large amount of experimental data accumulated over the past years and the ongoing high-quality measurements at such facilities as the Thomas Jefferson National Accelerator Facility (JLab), Mainz Microtron (MAMI), and others (for an overview of the modern developments, see the proceedings of the recent  $N^*$  Workshops [34–36]).

So far, the GBE CQM has been tested in calculating mesonic decays of resonances of light and strange baryons in a semirelativistic framework [37–39]. These studies have revealed that relativistic effects have a big influence on the results, both in an elementary-emission and a quark-pair-creation model of the decay operator. In the present work, we perform a covariant calculation of  $\pi$  and  $\eta$  decay modes of  $N$  and  $\Delta$  resonances using a rather simplified model for the decay operator. Our primary goal is to set up a fully relativistic (covariant) CQM formulation of mesonic decays; later on, one may still improve on the decay operator. In particular, we assume a decay operator in the point-form spectator

model (PFSM) with a pseudovector coupling. It has been seen in previous studies that such an operator includes effective many-body contributions due to the symmetry requirements of Poincaré invariance (especially in order to satisfy translational invariance of the transition amplitude) [40,41]. We produce the corresponding predictions for decay widths from the GBE CQM and analogous results from a CQM with a OGE hyperfine interaction, namely, the relativistic version of the Bhaduri-Cohler-Nogami CQM [42] as parametrized in Ref. [39]. In addition, a comparison is provided with results from the II CQM obtained with a similar (spectator-model) decay operator in a Bethe-Salpeter approach [19]. The relativistic results are also contrasted with several nonrelativistic and so-called semirelativistic calculations. Preliminary results have already been presented in proceedings contributions [43–45].

In Sec. II, we outline the theory for a covariant calculation of the mesonic decay widths from a relativistic CQM. In Secs. III and IV, we present the results of our calculation, discuss their qualitative and quantitative features, and compare them with the results of decay calculations from other models and/or approaches. In the Appendix, some details of the relativistic point-form calculation of mesonic baryon decays are given.

## II. THEORY

Generally, the decay width  $\Gamma$  of a particle is defined by

$$\Gamma = 2\pi\rho_f |F(i \rightarrow f)|^2, \quad (1)$$

where  $F(i \rightarrow f)$  is the transition amplitude and  $\rho_f$  is the phase-space factor. To get the total decay width, one has to average over the initial and sum over the final spin-isospin projections.

In nonrelativistic calculations, the strong decays of hadron resonances are treated with a transition amplitude that is not Lorentz invariant. Consequently, one is left with an arbitrary choice of the phase-space factor [26,32,46]. In the rest frame of the decaying resonance, either a purely nonrelativistic form,

$$\rho_f = \frac{M'm}{M}q, \quad (2)$$

or the relativistic form,

$$\rho_f = \frac{E'\omega_m}{M}q, \quad (3)$$

has been used. In Eq. (2),  $M$  is the mass of the initial resonance while  $M'$  and  $m$  are the masses of the final state and the emitted meson, respectively;  $q$  is the magnitude of the momentum transfer. Correspondingly, in Eq. (3),  $E'$  and  $\omega_m$  are the energies of the decay products. An alternative choice was made by Capstick and Roberts [30] using the phase-space factor

$$\rho_f = \frac{\tilde{M}'\tilde{m}}{\tilde{M}}q, \quad (4)$$

first introduced by Kokoski and Isgur [46] for meson decays. Here the quantities with the tilde represent some effective (parametrized) masses. Clearly, the particular choice of the phase-space factor has a pronounced effect on the final

results. The ambiguity concerning the phase-space factor is immediately resolved by imposing relativistic invariance on the formalism. This can evidently be done either along a relativistic field theory or in relativistic (Poincaré-invariant) quantum mechanics.

In the present work, we formulate a Poincaré-invariant description of the decay amplitude. Out of the possible forms of relativistic dynamics minimally affected by interactions [8,9] we make use of the point form. In this case, one has the advantage that only the four-momentum operator  $\hat{P}^\mu$  contains interactions. Consequently, the generators of the Lorentz transformations remain purely kinematic, and the theory is manifestly covariant [10]. The interactions are introduced into the (invariant) mass operator following the Bakamjian-Thomas construction [11]. Hereby the free mass operator  $\hat{M}_{\text{free}}$  is replaced by a full mass operator  $\hat{M}$  containing an interacting term  $\hat{M}_{\text{int}}$ :

$$\hat{M}_{\text{free}} \rightarrow \hat{M} = \hat{M}_{\text{free}} + \hat{M}_{\text{int}}. \quad (5)$$

The four-momentum operator is then defined by multiplying the mass operator  $\hat{M}$  by the four-velocity operator  $\hat{V}^\mu$

$$\hat{P}^\mu = \hat{M}\hat{V}^\mu. \quad (6)$$

In the point form, following the Bakamjian-Thomas construction, the four-velocity operator is kinematic and thus remains independent of interactions, i.e.,  $\hat{V}^\mu = \hat{V}_{\text{free}}^\mu$ . The eigenstates of the four-momentum operator  $\hat{P}^\mu$  are simultaneous eigenstates of the mass operator  $\hat{M}$  and the four-velocity operator  $\hat{V}^\mu$ ; this is simply a consequence of Poincaré invariance. For a given baryon state of mass  $M$  and total angular momentum  $J$  with  $z$  projection  $\Sigma$ , the eigenvalue problem of the mass operator reads

$$\hat{M}|V, M, J, \Sigma\rangle = M|V, M, J, \Sigma\rangle. \quad (7)$$

Here we have written the eigenstates in obvious notation as  $|V, M, J, \Sigma\rangle$ , where  $V$  indicates the four eigenvalues of  $V^\mu$ , of which only three are independent. Alternatively, we can express these eigenstates as

$$|V, M, J, \Sigma\rangle \equiv |P, J, \Sigma\rangle, \quad (8)$$

where  $P$  represents the four eigenvalues of  $\hat{P}^\mu$ , whose square gives the invariant mass operator.

For the actual calculation in the point form, it is advantageous to introduce a specific basis of free three-body states, the so-called velocity states, by

$$\begin{aligned} &|v; \vec{k}_1, \vec{k}_2, \vec{k}_3; \mu_1, \mu_2, \mu_3\rangle \\ &= U_{B(v)}|k_1, k_2, k_3; \mu_1, \mu_2, \mu_3\rangle \\ &= \sum_{\sigma_1, \sigma_2, \sigma_3} \prod_{i=1}^3 D_{\sigma_i \mu_i}^{\frac{1}{2}} \{R_W[k_i, B(v)]\} |p_1, p_2, p_3; \sigma_1, \sigma_2, \sigma_3\rangle. \end{aligned} \quad (9)$$

Here  $B(v)$ , with unitary representation  $U_{B(v)}$ , is a boost with four-velocity  $v$  on the free three-body states  $|k_1, k_2, k_3; \mu_1, \mu_2, \mu_3\rangle$  in the c.m. system, i.e., for which  $\sum \vec{k}_i = 0$ . The second line in Eq. (9) expresses the corresponding Lorentz transformation as acting on general three-body states  $|p_1, p_2, p_3; \sigma_1, \sigma_2, \sigma_3\rangle$ . The momenta  $p_i$  and  $k_i$

are related by  $p_i = B(v)k_i$ , where  $k_i = (\omega_i, \vec{k}_i)$ . The  $D^{\frac{1}{2}}$  are the spin- $\frac{1}{2}$  representation matrices of Wigner rotations  $R_W[k_i, B(v)]$ . It is advantageous to use the velocity-state basis (instead of the basis of general free three-body states) since in this case Lorentz transformations rotate all particles by the same angle, and the spin coupling can be done in the usual way [7,47]. Some further details concerning velocity states are given in the Appendix.

The relativistic transition amplitude for the mesonic decay of a baryon resonance  $|V, M, J, \Sigma\rangle$  to the nucleon ground state  $|V', M', J', \Sigma'\rangle$  is defined by the reduced matrix element of the mesonic decay operator  $\hat{D}_m$

$$\begin{aligned}
 F(i \rightarrow f) &= \langle V', M', J', \Sigma' | \hat{D}_{m,\text{rd}} | V, M, J, \Sigma \rangle \\
 &= \frac{2}{MM'} \sum_{\sigma_1 \sigma'_1} \sum_{\mu_i \mu'_i} \int d^3 \vec{k}_2 d^3 \vec{k}_3 d^3 \vec{k}'_2 d^3 \vec{k}'_3 \\
 &\quad \times \sqrt{\frac{(\sum \omega_i)^3}{2\omega_1 2\omega_2 2\omega_3}} \sqrt{\frac{(\sum \omega'_i)^3}{2\omega'_1 2\omega'_2 2\omega'_3}} \\
 &\quad \times \Psi_{M'J'\Sigma'}^*(\vec{k}'_i; \mu'_i) \prod_{\sigma'_i} D_{\sigma'_i \mu'_i}^{*\frac{1}{2}} \{R_W[k'_i; B(V')]\} \\
 &\quad \times \langle p'_1, p'_2, p'_3; \sigma'_1, \sigma'_2, \sigma'_3 | \hat{D}_{m,\text{rd}} \\
 &\quad \times | p_1, p_2, p_3; \sigma_1, \sigma_2, \sigma_3 \rangle \\
 &\quad \times \prod_{\sigma_i} D_{\sigma_i \mu_i}^{\frac{1}{2}} \{R_W[k_i; B(V)]\} \Psi_{MJ\Sigma}(\vec{k}_i; \mu_i).
 \end{aligned} \tag{10}$$

The wave functions  $\Psi_{M'J'\Sigma'}^*$  and  $\Psi_{MJ\Sigma}$  denote velocity-state representations of the baryon states  $\langle P', J', \Sigma' |$  and  $|P, J, \Sigma\rangle$ , respectively. For the decay operator  $\hat{D}_{m,\text{rd}}$ , we assume a spectator model with pseudovector coupling and express its matrix element by

$$\begin{aligned}
 &\langle p'_1, p'_2, p'_3; \sigma'_1, \sigma'_2, \sigma'_3 | \hat{D}_{m,\text{rd}} | p_1, p_2, p_3; \sigma_1, \sigma_2, \sigma_3 \rangle \\
 &= 3 \frac{ig_{qmqm}}{2m_1 (2\pi)^{\frac{3}{2}}} \sqrt{\frac{M^3 M'^3}{(\sum \omega_i)^3 (\sum \omega'_i)^3}} \bar{u}(p'_1, \sigma'_1) \\
 &\quad \times \gamma_5 \gamma^\mu \lambda_m u(p_1, \sigma_1) Q_\mu 2p_{20} \delta(\vec{p}_2 - \vec{p}'_2) \\
 &\quad \times 2p_{30} \delta(\vec{p}_3 - \vec{p}'_3) \delta_{\sigma_2 \sigma'_2} \delta_{\sigma_3 \sigma'_3},
 \end{aligned} \tag{11}$$

where  $g_{qmqm}$  is the meson-quark coupling constant,  $\lambda_m$  the flavor operator for the particular decay channel, and  $m_1$  the mass of the quark coupling to the generated meson. In the actual calculations for the theoretical predictions of the CQMs to be presented in the next section, the meson-quark coupling constant is assumed to be  $g_{qmqm}^2/4\pi = 0.67$ . This value is consistent with the one used in the parametrization of the GBE CQM (for both the  $\pi$ -quark and  $\eta$ -quark couplings) [5]. The dependence of the results for strong decay widths on the size of the meson-quark coupling constant is discussed in Sec. IV.

Equation (11) defines the spectator-model decay operator, here specifically in point form (PFSM). The transition amplitude in Eq. (10) is Poincaré invariant, and the overall momentum conservation  $P_\mu - P'_\mu = Q_\mu$  has already been exploited in the integral. Regarding the spectator model

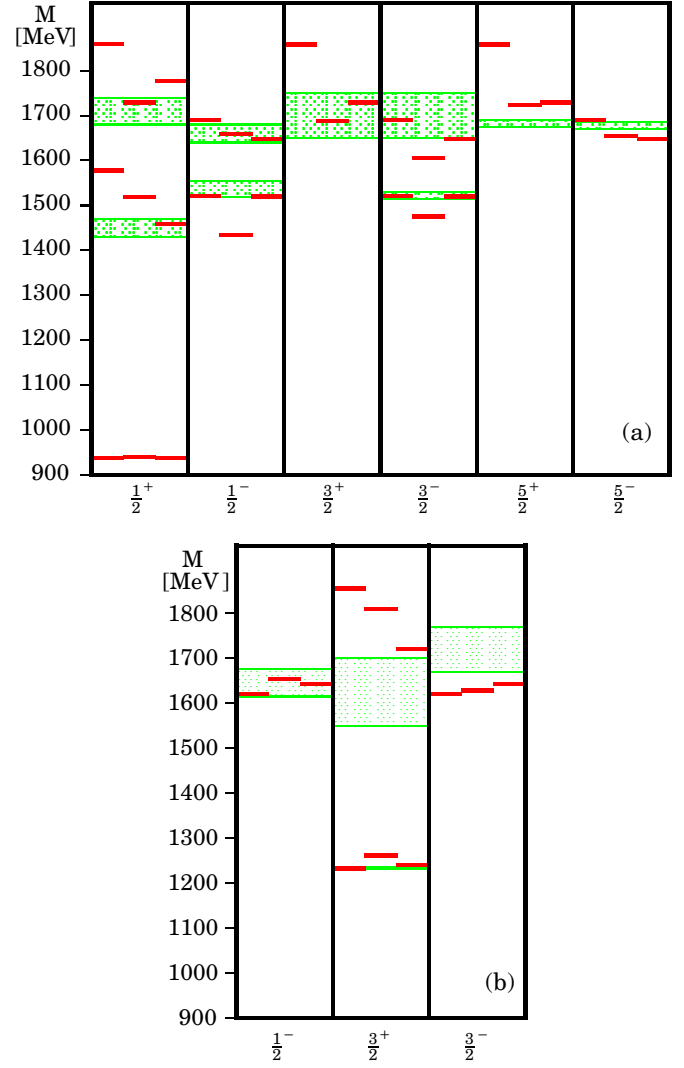


FIG. 1. (Color online) Nucleon (a) and  $\Delta$  (b) spectra from three different types of relativistic CQMs. In each column, the left horizontal lines represent the results of the relativistic version of the Bhaduri-Cohler-Nogami CQM [39], the middle ones of the II CQM (Version A) [2], and the right ones of the GBE CQM [5]. The shadowed boxes give the experimental data with their uncertainties after the latest compilation of the Particle Data Group [49].

of the decay operator, it should be noted that in PFSM the impulse delivered to the quark that emits the meson is not equal to the impulse delivered to the nucleon as a whole. However, the momentum transfer  $\vec{q}$  to this single quark is uniquely determined from the momentum  $Q$  transferred to the nucleon and the two spectator conditions [cf. Eq. (A.10)] [40]. The square-root normalization factor has been introduced in accordance with the previous PFSM studies in the electromagnetic case [13–15,18].

### III. DIRECT PREDICTIONS OF DECAY WIDTHS

It is well known that the underlying quark dynamics of CQMs has a pronounced effect on the baryon spectra [48]. In Fig. 1, we compare the  $N$  and  $\Delta$  spectra for three different

TABLE I. Covariant predictions for  $\pi$  decay widths by the GBE CQM [5] and the OGE CQM [39] along the PFSM in comparison to experiment [49] and a relativistic calculation for the II CQM along the Bethe-Salpeter approach [19]. In the last two columns, the nonrelativistic results from an EEM are given. In all cases, the theoretical resonance masses as predicted by the various CQMs have been used in the calculations.

Decay $\rightarrow N\pi$	Experiment (MeV)	Relativistic			Nonrel. EEM	
		GBE	OGE	II	GBE	OGE
$N(1440)$	$(227 \pm 18)_{-59}^{+70}$	33	68	38	6.7	27
$N(1520)$	$(66 \pm 6)_{-5}^{+9}$	17	16	38	38	37
$N(1535)$	$(67 \pm 15)_{-17}^{+28}$	90	119	33	554	1183
$N(1650)$	$(109 \pm 26)_{-3}^{+36}$	29	41	3	160	358
$N(1675)$	$(68 \pm 8)_{-4}^{+14}$	5.4	6.6	4	13	16
$N(1700)$	$(10 \pm 5)_{-3}^{+3}$	0.8	1.2	0.1	2.2	2.7
$N(1710)$	$(15 \pm 5)_{-5}^{+30}$	5.5	4.6	n/a	8.1	5.8
$\Delta(1232)$	$(119 \pm 1)_{-5}^{+5}$	37	32	62	89	84
$\Delta(1600)$	$(61 \pm 26)_{-10}^{+26}$	0.1	1.8	n/a	92	85
$\Delta(1620)$	$(38 \pm 8)_{-6}^{+8}$	11	15	4	77	178
$\Delta(1700)$	$(45 \pm 15)_{-10}^{+20}$	2.3	2.3	2	11	9.2

CQMs. While the  $N$ - $\Delta$  splittings are correct in all cases, only the GBE CQM succeeds simultaneously to reproduce the proper level ordering of positive- and negative-parity excitations. Now, it is interesting to learn how the CQMs with different dynamics predict the widths of various mesonic decay modes.

In Table I, we present the covariant predictions of the relativistic CQMs for  $\pi$  decay widths of  $N$  and  $\Delta$  resonances from the PFSM calculation. In this table, the theoretical masses of the baryon states as produced by the respective CQMs have been used. For the GBE CQM, only two decay widths, namely  $N(1535)$  and  $N(1710)$ , apparently coincide with experimental data within their error bars. All the others are smaller than experiment. In most cases, a considerable underestimation of the experimental data is found. The situation is similar for the OGE CQM, where only the  $N(1710)$  coincides with experiment. Again, all other predictions remain (considerably) smaller than the data. The situation is even worse for the II CQM, calculated in the Bethe-Salpeter approach [19], where none of the predictions strictly agree with experiment; each is too small, some by far. In general, all relativistic calculations, independently of the framework applied, show similar characteristics: They yield results always smaller than the experimental data or at most reaching their values from below.

For comparison with nonrelativistic results, we applied the elementary emission model (EEM), which can be viewed as the nonrelativistic analog of the spectator model used for our covariant calculations. The comparison of the relativistic and nonrelativistic results in Table I tells us that there are huge differences between them. While there is a common trend in the relativistic results (practically none of the predictions overshoot the data), the nonrelativistic decay widths scatter below and above the experimental values. Incidentally, for the

nonrelativistic results, agreement with experiment is found in more cases than for the relativistic ones. However, this observation should not be interpreted as a better quality of the nonrelativistic results. From the viewpoint of theory, the relativistic calculations are much more appealing. In particular, the corresponding predictions are covariant. Furthermore, the fact that they generally underestimate the data may turn out to be an advantage, especially when a more complete decay operator is employed than the simple spectator model used here.

In the literature, results for decay widths are often calculated employing phenomenological resonance masses instead of theoretical ones (as predicted by the respective CQM). Therefore, in Table II we also give the decay widths calculated with the physical resonance masses (but with the same CQM wave functions as before). For the GBE CQM, only slight variations are seen as compared to Table I. This is not surprising, since the GBE CQM yields a rather good reproduction of the experimental resonance masses. For the OGE CQM, some bigger deviations are observed, especially in case of the positive-parity resonances  $N(1440)$ ,  $N(1710)$ , and  $\Delta(1600)$ , where differences of more than 50% may occur. For the OGE CQM, the mass-shift effect is also visible for the negative-parity resonance  $\Delta(1700)$ . Also the nonrelativistic results exhibit an analogous behavior. We learn that the resonance masses have a pronounced influence on the magnitudes of the decay widths. For a given resonance (and a given wave function), the decay width will come out bigger the larger its mass. It is therefore an essential prerequisite that any CQM reproduces the excitation spectra in fair agreement with experiment.

By comparing the GBE and OGE columns in Table II one can see the influences of different wave functions on the decay widths (since here the employed resonance masses are the

TABLE II. Same as Table I, but with experimental resonance masses instead, of theoretical ones.

Decay $\rightarrow N\pi$	Experiment (MeV)	Relativistic		Nonrel. EEM	
		GBE	OGE	GBE	OGE
$N(1440)$	$(227 \pm 18)_{-59}^{+70}$	30	37	6.2	14
$N(1520)$	$(66 \pm 6)_{-5}^{+9}$	17	16	38	36
$N(1535)$	$(67 \pm 15)_{-17}^{+28}$	93	123	574	1230
$N(1650)$	$(109 \pm 26)_{-3}^{+36}$	29	38	160	332
$N(1675)$	$(68 \pm 8)_{-4}^{+14}$	6.0	6.2	15	15
$N(1700)$	$(10 \pm 5)_{-3}^{+3}$	0.9	1.2	2.9	2.9
$N(1710)$	$(15 \pm 5)_{-5}^{+30}$	4.1	2.3	6.0	3.2
$\Delta(1232)$	$(119 \pm 1)_{-5}^{+5}$	34	32	81	84
$\Delta(1600)$	$(61 \pm 26)_{-10}^{+26}$	0.1	0.5	56	30
$\Delta(1620)$	$(38 \pm 8)_{-6}^{+8}$	10	15	75	178
$\Delta(1700)$	$(45 \pm 15)_{-10}^{+20}$	2.9	3.1	14	15

same in both cases, namely, the experimental ones). Obviously the different components in the respective wave functions also can have a respectable effect. For example, the OGE wave function produces a considerably larger  $\pi$  decay width for  $N(1535)$  than the GBE. A similar behavior is found for  $\Delta(1620)$  and to some extent also for  $N(1650)$ . All of these resonances have  $J^P = \frac{1}{2}^-$ . The OGE result is also higher in the case of the Roper resonances  $N(1440)$  and  $\Delta(1600)$ . All the other  $\pi$  decay widths have very similar magnitudes for both types of wave functions. Only in the case of the  $N(1710)$  resonance does the result with the GBE wave function come out appreciably larger than with the OGE. An analogous behavior is found in the nonrelativistic results for the EEM [with the exception of  $\Delta(1600)$ ].

It is interesting to examine the theoretical results from a different viewpoint. In Table III, we present the covariant

predictions of the various CQMs as percentage values relative to the experimental  $\pi$  decay widths. Evidently, since all of the predictions tend to be too small by their absolute values, these percentages also turn out too small. The only exception is  $N(1535)$ , in which case, an appreciable percentage is reached (evidently because the theoretical prediction is of the magnitude of the experimental decay width). If we look at the corresponding experimental  $N\pi\pi$  branching ratio, incidentally, we observe that it is very small. On the other hand, the  $N\pi\pi$  branching ratios are observed to be quite large in other cases, such as  $N(1675)$ ,  $N(1700)$ ,  $\Delta(1600)$ , and  $\Delta(1700)$ . Here, they may become 60–90%. Interestingly, in these cases the theoretical  $\pi$  decay widths assume only very small percentages of the experimental decay widths. While the situation is not as clearcut with respect to the  $N(1440)$ ,  $N(1520)$ , and  $N(1710)$  resonances—they appear to

TABLE III. Covariant predictions for  $\pi$  decay widths of the GBE, OGE, and II CQMs (as in Table I) presented as percentages of the experimental  $\pi$  decay widths in comparison to experimental  $N\pi\pi$  branching ratios.

Decays $\rightarrow N\pi$	$J^P$	Experiment (MeV)	Relativistic			% of Exp. Width			Experimental $N\pi\pi$ Branching Ratio
			GBE	OGE	II	GBE	OGE	II	
$N(1440)$	$\frac{1}{2}^+$	$(227 \pm 18)_{-59}^{+70}$	33	68	38	14	30	17	30–40%
$N(1520)$	$\frac{3}{2}^-$	$(66 \pm 6)_{-5}^{+9}$	17	16	38	26	24	58	40–50%
$N(1535)$	$\frac{1}{2}^-$	$(67 \pm 15)_{-17}^{+28}$	90	119	33	134	178	49	1–10%
$N(1650)$	$\frac{1}{2}^-$	$(109 \pm 26)_{-3}^{+36}$	29	41	3	27	38	3	10–20%
$N(1675)$	$\frac{5}{2}^-$	$(68 \pm 8)_{-4}^{+14}$	5.4	6.6	4	8	10	6	50–60%
$N(1700)$	$\frac{3}{2}^-$	$(10 \pm 5)_{-3}^{+3}$	0.8	1.2	0.1	8	12	1	85–95%
$N(1710)$	$\frac{1}{2}^+$	$(15 \pm 5)_{-5}^{+30}$	5.5	4.6	n/a	37	31	n/a	40–90%
$\Delta(1232)$	$\frac{3}{2}^+$	$(119 \pm 1)_{-5}^{+5}$	37	32	62	31	27	52	n/a
$\Delta(1600)$	$\frac{3}{2}^+$	$(61 \pm 26)_{-10}^{+26}$	0.07	1.8	n/a	$\approx 0$	3	n/a	75–90%
$\Delta(1620)$	$\frac{1}{2}^-$	$(38 \pm 8)_{-6}^{+8}$	11	15	4	29	39	11	70–80%
$\Delta(1700)$	$\frac{3}{2}^-$	$(45 \pm 15)_{-10}^{+20}$	2.3	2.3	2	5	5	4	80–90%

TABLE IV. Covariant predictions for  $\eta$  decay widths by the GBE CQM [5] and the OGE CQM [39] along the PFSM in comparison to experiment [49]. In the last two columns, the nonrelativistic results from an EEM are given. In all cases, the theoretical resonance masses as predicted by the various CQMs have been used in the calculations.

Decay $\rightarrow N\eta$	Experiment (MeV)	Relativistic		Nonrel. EEM	
		GBE	OGE	GBE	OGE
$N(1520)$	$(0.28 \pm 0.05)_{-0.01}^{+0.03}$	0.04	0.04	0.04	0.04
$N(1535)$	$(64 \pm 19)_{-28}^{+28}$	30	39	127	236
$N(1650)$	$(10 \pm 5)_{-1}^{+4}$	71	109	285	623
$N(1675)$	$(0 \pm 1.5)_{-0.1}^{+0.3}$	0.6	0.9	1.1	1.8
$N(1700)$	$(0 \pm 1)_{-0.5}^{+0.5}$	0.2	0.4	0.2	0.3
$N(1710)$	$(6 \pm 1)_{-4}^{+11}$	1.0	1.6	2.9	9.3

be intermediate in this behavior—one would have expected the  $N(1650)$  decay width to be larger. Its  $N\pi\pi$  branching ratio remains smaller than 20%. In this case, however, we should also observe that the  $N\eta$  decay width is of an appreciable magnitude experimentally; in addition, it becomes far too large in the CQMs (see the discussion below).

In the context of this comparison, looking at the  $\pi$  decay widths relative to the magnitudes of the branching ratios to other decay channels, we identify a principal shortcoming of the present approach to mesonic decays. A single-channel decay operator appears to be insufficient, and a more complete decay mechanism, including channel couplings, is called for.

In Table IV, we also present the covariant predictions of the GBE and OGE CQMs for  $\eta$  decay widths. Again the theoretical resonance masses were employed, and a comparison to the nonrelativistic EEM is given. In the  $\eta$  decay mode, only two resonances,  $N(1535)$  and  $N(1650)$ , show a sizable decay width. This behavior is exactly met by the CQMs. In particular, the  $N(1535)$  decay width is reproduced within the experimental error bars by both relativistic CQMs. One should recall that this is the same resonance for which the  $\pi$  decay widths were reproduced best, practically in agreement with experiment (see Table I). The experimental  $\eta$  decay width of  $N(1650)$  is overshoot by both CQMs. These deficiencies might be connected with the ones in the  $\pi$  decay widths, which came out unexpectedly small. Again large differences are found between the covariant predictions and the nonrelativistic EEM results.

Table V shows the  $\eta$  decay widths calculated with experimental resonance masses. Compared with the data in Table IV, the mass-shift effects are clearly visible (in the same manner as for the  $\pi$  decay widths above). Again, the comparison of the GBE and OGE columns in Table V shows the influences of the different CQM wave functions. For both the  $N(1535)$  and the  $N(1650)$ , the OGE wave function leads to higher values for the  $\eta$  decay widths. In all other cases, the predictions are very similar (and small). A completely analogous behavior is found for the nonrelativistic EEM.

In this section, we have presented covariant results for  $\pi$  and  $\eta$  decay widths as direct predictions by the relativistic GBE and OGE CQMs with the PFSM decay operator. We have discussed them in comparison with experiment and (as far as existing) to covariant results by the II CQM. Huge differences were found as compared with nonrelativistic predictions along the EEM.

#### IV. COMPARISON WITH OTHER DECAY CALCULATIONS

Let us now look at our results in the light of mesonic decay calculations existing in the literature. We used the EEM in the comparisons made in the previous section as a (nonrelativistic) reference model, since it serves as the best analog of the relativistic PFSM. However, past studies showed that the EEM is not sufficiently sophisticated to provide a reasonable description of the mesonic decays. A more elaborate decay

TABLE V. Same as Table III, but with experimental resonance masses instead of theoretical ones.

Decay $\rightarrow N\eta$	Experiment (MeV)	Relativistic		Nonrel. EEM	
		GBE	OGE	GBE	OGE
$N(1520)$	$(0.28 \pm 0.05)_{-0.01}^{+0.03}$	0.04	0.03	0.05	0.04
$N(1535)$	$(64 \pm 19)_{-28}^{+28}$	36	46	155	282
$N(1650)$	$(10 \pm 5)_{-1}^{+4}$	72	95	288	543
$N(1675)$	$(0 \pm 1.5)_{-0.1}^{+0.3}$	0.8	0.8	1.6	1.5
$N(1700)$	$(0 \pm 1)_{-0.5}^{+0.5}$	0.4	0.4	0.4	0.3
$N(1710)$	$(6 \pm 1)_{-4}^{+11}$	1.0	1.4	2.2	4.6

TABLE VI. Scaled predictions for  $\pi$  decay widths by the GBE CQM [5] and OGE CQM [39] along the PFSM in comparison to results existing in the literature from calculations along PCMs by Stancu and Stassart [28] (SS), by Capstick and Roberts [30] (CR), and by Theussl, Wagenbrunn, Desplanques, and Plessas [39] (TWDP).

Decay $\rightarrow N\pi$	Experiment [49] (MeV)	PFSM		PCM		
		GBE	OGE	SS	CR	TWDP
$N(1440)$	$(227 \pm 18)_{-59}^{+70}$	106	253	433	493	517
$N(1520)$	$(66 \pm 6)_{-5}^{+9}$	55	60	71	100	131
$N(1535)$	$(67 \pm 15)_{-17}^{+28}$	290	443	40	207	336
$N(1650)$	$(109 \pm 26)_{-3}^{+36}$	93	153	5.3	115	53
$N(1675)$	$(68 \pm 8)_{-4}^{+14}$	17	25	31	33	34
$N(1700)$	$(10 \pm 5)_{-3}^{+3}$	2.6	4.5	17	36	6
$N(1710)$	$(15 \pm 5)_{-5}^{+30}$	18	17	3.2	12	54
$\Delta(1232)$	$(119 \pm 1)_{-5}^{+5}$	119	119	115	104	120
$\Delta(1600)$	$(61 \pm 26)_{-10}^{+26}$	0.2	6.7	0.04	40	43
$\Delta(1620)$	$(38 \pm 8)_{-6}^{+8}$	35	56	0.4	21	26
$\Delta(1700)$	$(45 \pm 15)_{-10}^{+20}$	7.4	8.6	23	27	28

mechanism is furnished by the so-called pair-creation model (PCM). Corresponding studies were performed, for example, by Stancu and Stassart [28], Capstick and Roberts [30], and by Theussl, Wagenbrunn, Desplanques, and Plessas [39]. In all of these calculations, some adjustments or additional parametrizations were applied on top of the direct predictions by the CQMs employed. For instance, one introduced by phenomenological parametrizations different forms and extensions of the interaction (meson-creation) vertex or one adjusted the pair-creation strength. Mostly the size of the  $\pi$  decay width of the  $\Delta(1232)$  was used as a reference. In the works of SS and CR, additional input was advocated to fit further ingredients in the calculations that were not determined by the underlying CQM.

Clearly, since the  $\pi$  decay width of the  $\Delta(1232)$  was always used as a constraint in the fits, this quantity is usually realistic in the PCM calculations. We have therefore decided to scale the PFSM results in an analogous manner by adjusting the quark-pion coupling in the decay operator so as to reproduce the  $\Delta(1232)$  in coincidence with experiment (this corresponds to a value  $g_{qqm}^2/4\pi = 2.15$  in the case of the GBE CQM and  $g_{qqm}^2/4\pi = 2.49$  in the case of the OGE CQM). Table VI gives the corresponding comparison of the results. Evidently, all the PFSM decay widths are now scaled to larger values with the consequence that the comparison to experiment is much improved. In particular, for the GBE CQM, the  $\pi$  decay widths of  $N(1520)$ ,  $N(1650)$ ,  $N(1700)$ ,  $N(1710)$ , and  $\Delta(1620)$  now appear to be correct. One is therefore tempted to accept that the tuning of the quark-pion coupling in the PFSM decay operator improves the description of the decay widths. The PFSM calculation is now at least of a similar overall quality in reproducing the data as the PCMs. While there is no common trend in the PCM calculations by the different groups, the scaled PFSM decay widths are either

correct or still remain smaller than the experimental data, with the notable exception of  $N(1535)$ . The  $N(1535)$  decay width that was correct before (see the previous section) is now grossly overestimated. Consequently, by tuning the quark-pion coupling strength, one can influence the predictions for the decay widths.

We have also studied the dependence of the results on the size of the quark-pion coupling constant in more detail. It is well known that the quark-meson coupling can vary in a certain range depending on the way it is deduced from the experimentally measured nucleon-meson couplings (which also have uncertainties). In Ref. [6], an allowed range of the quark-pion coupling constant of  $0.67 \lesssim g_{qq\pi}^2/4\pi \lesssim 1.19$  was determined. In the actual parametrization of the GBE CQM the value  $g_{qq\pi}^2/4\pi = 0.67$  was employed; the same value was used for the results in the previous section for consistency reasons. If we now take the liberty of changing the strength of the quark-pion coupling in the decay operator of Eq. (11), we can scale it such that the decay widths are all increased from the results in Table I. Following the principle that neither one of the decay widths exceeds the experimental range, we can allow  $g_{qq\pi}^2/4\pi$  to assume the value of 0.82. In this case the decay width of  $N(1535)$ , which results largest as compared to experiment, is still within the experimental range (cf. Table VII). Evidently, all other decay widths get increased too and thus come closer to the experimental values. If we push the value of  $g_{qq\pi}^2/4\pi$  to the highest allowed value of about 1.2, the results in the last column of Table VII are obtained. Here, only the decay width of  $N(1535)$  is overshoot, while all the other ones are still improved.

Regarding the PCM calculations discussed above, one should also bear in mind that they are not covariant. In view of the large relativistic effects found in the PFSM study, one must take the corresponding results with some doubt. We conclude

TABLE VII. Predictions for  $\pi$  decay widths by the GBE CQM [5] and OGE CQM [39] along the PFSM for different magnitudes of the quark-meson coupling constant  $g_{qq\pi}$ .

Decay $\rightarrow N\pi$	Experiment	$\frac{g_{qq\pi}^2}{4\pi} = 0.67$		$\frac{g_{qq\pi}^2}{4\pi} = 0.82$		$\frac{g_{qq\pi}^2}{4\pi} = 1.19$	
		GBE	OGE	GBE	OGE	GBE	OGE
$N(1440)$	$(227 \pm 18)_{-59}^{+70}$	33	68	40	83	64	131
$N(1520)$	$(66 \pm 6)_{-5}^{+9}$	17	16	21	20	33	31
$N(1535)$	$(67 \pm 15)_{-17}^{+28}$	90	119	110	145	174	230
$N(1650)$	$(109 \pm 26)_{-3}^{+36}$	29	41	35	50	56	79
$N(1675)$	$(68 \pm 8)_{-4}^{+14}$	5.4	6.6	6.6	8.1	10	13
$N(1700)$	$(10 \pm 5)_{-3}^{+3}$	0.8	1.2	1.0	1.5	1.5	2.3
$N(1710)$	$(15 \pm 5)_{-5}^{+30}$	5.5	4.6	6.7	5.6	11	8.9
$\Delta(1232)$	$(119 \pm 1)_{-5}^{+5}$	37	32	45	39	71	62
$\Delta(1600)$	$(61 \pm 26)_{-10}^{+26}$	0.1	1.8	0.1	2.2	0.2	3.5
$\Delta(1620)$	$(38 \pm 8)_{-6}^{+8}$	11	15	13	18	21	29
$\Delta(1700)$	$(45 \pm 15)_{-10}^{+20}$	2.3	2.3	2.8	2.8	4.4	4.4

that considerable efforts are still needed to find the proper decay mechanism/operator. Of course, such studies must be done in a fully relativistic framework.

## V. SUMMARY

We have presented covariant predictions for  $\pi$  and  $\eta$  decay widths of  $N$  and  $\Delta$  resonances by two different types of relativistic CQMs. The results have been obtained by calculating the transition matrix elements of the PFSM decay operator directly with the wave functions of the respective CQMs, and no additional parametrization has been introduced *a priori*. In general, the relativistic predictions usually underestimated the experimental data. These findings are congruent with the ones recently made in a Bethe-Salpeter approach [19]. The reproduction of the experimental data by the CQMs can be improved by an additional tuning of the quark-meson coupling in the PFSM decay operator.

We have also determined large relativistic effects in the decay widths. Thus it appears mandatory to perform any (future) investigation of mesonic decays in a relativistic framework. In this respect, Poincaré-invariant relativistic quantum mechanics provides a viable approach to treating CQMs.

Upon a closer examination of the  $\pi$  decay widths, we detected a certain correlation of their magnitudes to the  $N\pi\pi$  branching ratios. Whenever the latter are large, the theoretical decay widths are far too small. We take this finding as a hint to a principal shortcoming of the applied decay mechanism. Very probably a more elaborate decay operator that includes channel couplings is needed. In this regard, point-form relativistic quantum mechanics opens the way toward a covariant treatment of a coupled-channel system. Corresponding investigations have already been performed in the meson sector [50,51]. It will be an ambitious goal to construct a coupled-channel theory also for baryons.

## ACKNOWLEDGMENTS

This work was supported by the Austrian Science Fund (Project P16945). We are grateful to Bianka Sengl for an independent check of some of the results.

## APPENDIX: DETAILS OF THE CALCULATION

Here we explain several details relevant to the evaluation of the decay widths from the matrix elements of the decay operator. The notation follows the one of Ref. [53] utilizing relativistically invariant scalar products of states, spinors, etc.

The velocity states defined in Eq. (9) have the following completeness relation

$$\mathbf{1} = \sum_{\mu_1\mu_2\mu_3} \int \frac{d^3v}{v_0} \frac{d^3k_2}{2\omega_2} \frac{d^3k_3}{2\omega_3} \frac{(\omega_1 + \omega_2 + \omega_3)^3}{2\omega_1} \times |v; \vec{k}_1, \vec{k}_2, \vec{k}_3; \mu_1, \mu_2, \mu_3\rangle \langle v; \vec{k}_1, \vec{k}_2, \vec{k}_3; \mu_1, \mu_2, \mu_3|, \quad (\text{A.1})$$

and the corresponding orthogonality relation reads

$$\begin{aligned} & \langle v; \vec{k}_1, \vec{k}_2, \vec{k}_3; \mu_1, \mu_2, \mu_3 | v'; \vec{k}'_1, \vec{k}'_2, \vec{k}'_3; \mu'_1, \mu'_2, \mu'_3 \rangle \\ &= \frac{2\omega_1 2\omega_2 2\omega_3}{(\omega_1 + \omega_2 + \omega_3)^3} \delta_{\mu_1\mu'_1} \delta_{\mu_2\mu'_2} \delta_{\mu_3\mu'_3} \\ & \times v_0 \delta^3(\vec{v} - \vec{v}') \delta^3(\vec{k}_2 - \vec{k}'_2) \delta^3(\vec{k}_3 - \vec{k}'_3). \end{aligned} \quad (\text{A.2})$$

For the actual calculation, one needs the overlap matrix element

$$\begin{aligned} & \langle p'_1, p'_2, p'_3; \sigma'_1, \sigma'_2, \sigma'_3 | v; \vec{k}_1, \vec{k}_2, \vec{k}_3; \mu_1, \mu_2, \mu_3 \rangle \\ &= \prod_{i=1}^3 D_{\sigma'_i\mu_i}^{\frac{1}{2}} \{R_W[k_i, B(v)]\} 2p_i^0 \delta(\vec{p}_i - \vec{p}'_i). \end{aligned} \quad (\text{A.3})$$



The velocity-state representation of the baryon eigenstates of Eq. (8) then becomes

$$\langle v; \vec{k}_1, \vec{k}_2, \vec{k}_3; \mu_1, \mu_2, \mu_3 | V, M, J, \Sigma \rangle = \frac{\sqrt{2}}{M} v_0 \delta^3(\vec{v} - \vec{V}) \sqrt{\frac{2\omega_1 2\omega_2 2\omega_3}{(\omega_1 + \omega_2 + \omega_3)^3}} \Psi_{MJ\Sigma}(\vec{k}_i; \mu_i). \quad (\text{A.4})$$

This representation has the advantage of separating the motion of the system as a whole and the internal motion. The latter is described by the wave function  $\Psi_{MJ\Sigma}(\vec{k}_i; \mu_i)$ , which is also the rest-frame wave function. It depends on the individual spin projections  $\mu_1, \mu_2, \mu_3$  and on the individual momenta  $\vec{k}_1, \vec{k}_2, \vec{k}_3$ , restricted by  $\sum \vec{k}_i = 0$ ; it is normalized as

$$\delta_{MM'} \delta_{JJ'} \delta_{\Sigma\Sigma'} = \sum_{\mu_1 \mu_2 \mu_3} \int d^3 k_2 d^3 k_3 \times \Psi_{M'J'\Sigma'}^*(\vec{k}_i; \mu_i) \Psi_{MJ\Sigma}(\vec{k}_i; \mu_i). \quad (\text{A.5})$$

These wave functions are obtained by solving the eigenvalue problem of the interacting mass operator  $\hat{M}$ .

In the practical calculation of decays, one adheres to a special frame of reference. For convenience, one chooses the rest frame of the decaying resonance with the momentum transfer in  $z$  direction [53]. In the chosen reference frame, the boosts to be applied in the transition matrix element are given by

$$B(v_{in}) = \mathbf{1}_4 \quad (\text{A.6})$$

$$B(v_f) = \begin{pmatrix} \cosh \Delta & 0 & 0 & \sinh \Delta \\ 0 & 1 & 0 & 0 \\ 0 & 0 & 1 & 0 \\ \sinh \Delta & 0 & 0 & \cosh \Delta \end{pmatrix} \quad (\text{A.7})$$

where

$$\sinh \Delta = \frac{Q}{M}, \quad (\text{A.8})$$

$$\cosh \Delta = \sqrt{1 + \frac{Q^2}{M^2}}, \quad (\text{A.9})$$

and  $M$  is the mass of the nucleon.

With these boost transformations, we can rewrite the spectator conditions in Eq. (11) as

$$2p_i^0 \delta(\vec{p}_i - \vec{p}'_i) = 2\omega_i^0 \delta[B^{-1}(v_f)B(v_{in})\vec{k}_i - \vec{k}'_i]. \quad (\text{A.10})$$

For the active quark, one obtains

$$\begin{aligned} & \sum_{\sigma_i \sigma'_i} D_{\sigma'_i \mu'_i}^{*\frac{1}{2}} \{R_W[k'_i; B(v_f)]\} \bar{u}(p'_i, \sigma'_i) \gamma_5 \gamma^\mu \lambda_m \\ & \times u(p_i, \sigma_i) D_{\sigma_i \mu_i}^{\frac{1}{2}} \{R_W[k_i; B(v_{in})]\} \\ & = \bar{u}(k'_1, \mu'_1) S[B^{-1}(v_f)] \gamma_5 \gamma^\mu \lambda_m S[B(v_{in})] u(k_1, \mu_1) \\ & = \bar{u}(k'_1, \mu'_1) \left( \cosh \frac{\Delta}{2} - \gamma_0 \gamma_3 \sinh \frac{\Delta}{2} \right) \gamma_5 \gamma^\mu \lambda_m u(k_1, \mu_1), \end{aligned} \quad (\text{A.11})$$

where the boost transformations on the Dirac spinors, represented by  $S[B^{-1}(v_f)]$  and  $S[B(v_{in})]$ , respectively, have been written out explicitly in the last line. These expressions are to be used in the evaluation of the matrix element of the decay operator, where the quark spinors can be represented conveniently in the form

$$u(k_1, \mu_1) = \sqrt{\omega_1 + m_q} \begin{pmatrix} 1 \\ \frac{\sigma_1 \vec{k}_1}{\omega_1 + m_q} \end{pmatrix} \chi(\mu_1), \quad (\text{A.12})$$

with  $m_q$  the quark mass and the Pauli spinors  $\chi(\mu_1)$  normalized to unity.

- 
- [1] S. Capstick and N. Isgur, Phys. Rev. D **34**, 2809 (1986).  
[2] U. Loering, B. C. Metsch, and H. R. Petry, Eur. Phys. J. A **10**, 395 (2001).  
[3] U. Loering, B. C. Metsch, and H. R. Petry, Eur. Phys. J. A **10**, 447 (2001).  
[4] L. Y. Glozman and D. O. Riska, Phys. Rep. **268**, 263 (1996).  
[5] L. Y. Glozman, W. Plessas, K. Varga, and R. F. Wagenbrunn, Phys. Rev. D **58**, 094030 (1998).  
[6] L. Y. Glozman, Z. Papp, W. Plessas, K. Varga, and R. F. Wagenbrunn, Phys. Rev. C **57**, 3406 (1998).  
[7] B. D. Keister and W. N. Polyzou, Adv. Nucl. Phys. **20**, 225 (1991).  
[8] P. Dirac, Rev. Mod. Phys. **21**, 392 (1949).  
[9] H. Leutwyler and J. Stern, Ann. Phys. (NY) **112**, 94 (1978).  
[10] W. H. Klink, Phys. Rev. C **58**, 3587 (1998).  
[11] B. Bakamjian and L. H. Thomas, Phys. Rev. **92**, 1300 (1953).  
[12] F. Cardarelli, E. Pace, G. Salme, and S. Simula, Phys. Lett. **B357**, 267 (1995).  
[13] R. F. Wagenbrunn, S. Boffi, W. Klink, W. Plessas, and M. Radici, Phys. Lett. **B511**, 33 (2001).  
[14] L. Y. Glozman, M. Radici, R. Wagenbrunn, S. Boffi, W. Klink, and W. Plessas, Phys. Lett. **B516**, 183 (2001).  
[15] S. Boffi, L. Glozman, W. Klink, W. Plessas, M. Radici, and R. Wagenbrunn, Eur. Phys. J. A **14**, 17 (2002).  
[16] D. Merten, U. Loering, K. Kretzschmar, B. Metsch, and H. R. Petry, Eur. Phys. J. A **14**, 477 (2002).  
[17] B. Julia-Diaz, D. O. Riska, and F. Coester, Phys. Rev. C **69**, 035212 (2004).  
[18] K. Berger, R. F. Wagenbrunn, and W. Plessas, Phys. Rev. D **70**, 094027 (2004).  
[19] B. Metsch, AIP Conf. Proc. **717**, 646 (2004).  
[20] C. Becchi and G. Morpurgo, Phys. Rev. **149**, 1284 (1966).  
[21] A. N. Mitra and M. Ross, Phys. Rev. **158**, 1630 (1967).  
[22] D. Faiman and A. W. Hendry, Phys. Rev. **173**, 1720 (1968).  
[23] D. Faiman and A. W. Hendry, Phys. Rev. **180**, 1609 (1969).  
[24] R. P. Feynman, M. Kislinger, and F. Ravndal, Phys. Rev. D **3**, 2706 (1971).  
[25] R. Koniuk and N. Isgur, Phys. Rev. D **21**, 1868 (1980).  
[26] S. Kumano and V. R. Pandharipande, Phys. Rev. D **38**, 146 (1988).  
[27] A. LeYaouanc, L. Oliver, O. Pene, and J. Raynal, *Hadron Transitions in the Quark Model* (Gordon and Breach, New York, 1988).  
[28] Fl. Stancu and P. Stassart, Phys. Rev. D **38**, 233 (1988).

- [29] Fl. Stancu and P. Stassart, Phys. Rev. D **39**, 343 (1989).
- [30] S. Capstick and W. Roberts, Phys. Rev. D **47**, 1994 (1993).
- [31] S. Capstick and W. Roberts, Phys. Rev. D **49**, 4570 (1994).
- [32] P. Geiger and E. S. Swanson, Phys. Rev. D **50**, 6855 (1994).
- [33] E. S. Ackleh, T. Barnes, and E. S. Swanson, Phys. Rev. D **54**, 6811 (1996).
- [34] D. Drechsel and L. Tiator, eds., *NSTAR2001, Proceedings of the Workshop on the Physics of Excited Nucleons, Mainz* (World Scientific, Singapore, 2001).
- [35] S. A. Dytman and E. S. Swanson, eds., *NSTAR2002, Proceedings of the Workshop on the Physics of Excited Nucleons, Pittsburgh, USA* (World Scientific, Singapore, 2003).
- [36] J. P. Bocquet, V. Kuznetsov, and D. Rebreyend, eds., *NSTAR2004, Proceedings of the Workshop on the Physics of Excited Nucleons, Grenoble* (World Scientific, Singapore, 2004).
- [37] A. Krassnigg, W. Plessas, L. Theussl, R. F. Wagenbrunn, and K. Varga, Few-Body Syst. Suppl. **10**, 391 (1999).
- [38] W. Plessas, A. Krassnigg, L. Theussl, R. F. Wagenbrunn, and K. Varga, Few-Body Syst. Suppl. **11**, 29 (1999).
- [39] L. Theussl, R. F. Wagenbrunn, B. Desplanques, and W. Plessas, Eur. Phys. J. A **12**, 91 (2001).
- [40] T. Melde, L. Canton, W. Plessas, and R. F. Wagenbrunn (2004), Eur. Phys. J. A., in print, hep-ph/0411322.
- [41] T. Melde, L. Canton, W. Plessas, and R. F. Wagenbrunn (2004), in 'Theoretical Nuclear Physics in Italy' (Proceedings of the 10<sup>th</sup> Conf. on Problems in Theor. Nucl. Phys., Cortona, 2004) edited by S. Boffi *et al.* (World Scientific, Singapore, 2005), p. 213.
- [42] R. K. Bhaduri, L. E. Cohler, and Y. Nogami, Phys. Rev. Lett. **44**, 1369 (1980).
- [43] T. Melde, W. Plessas, and R. F. Wagenbrunn, Few-Body Syst. Suppl. **14**, 37 (2003).
- [44] T. Melde, W. Plessas, and R. F. Wagenbrunn, in *NSTAR2004, Proceedings of the Workshop on the Physics of Excited Nucleons, Grenoble* edited by J. P. Bocquet, V. Kuznetsov, and D. Rebreyend (World Scientific, Singapore, 2004), p. 355.
- [45] T. Melde, L. Canton, W. Plessas, and R. F. Wagenbrunn, in *Proceedings of the Mini-Workshop on Quark Dynamics, Bled, 2004* (Univ. Ljubljana, Slovenia, 2004), p. 43.
- [46] R. Kokoski and N. Isgur, Phys. Rev. D **35**, 907 (1987).
- [47] W. H. Klink, Phys. Rev. C **58**, 3617 (1998).
- [48] W. Plessas, Few-Body Syst. Suppl. **15**, 139 (2003).
- [49] S. Eidelman *et al.*, Phys. Lett. **B592**, 1 (2004); URL <http://pdg.lbl.gov>.
- [50] A. Krassnigg, W. Schweiger, and W. H. Klink, Phys. Rev. C **67**, 064003 (2003).
- [51] A. Krassnigg, submitted to Phys. Rev. C., nucl-th/0412017.
- [52] F. J. Yndurain, *Relativistic Quantum Mechanics and Introduction to Field Theory* (Springer Verlag, Berlin, 1996).
- [53] We emphasize that the final results are independent of the frame of reference since the PFSM calculation is manifestly covariant.